Am J Transl Res 2021;13(8):8952-8964
www.ajtr.org /ISSN:1943-8141/AJTR0133368

Original Article

Matrix mapping of different idiopathic right ventricular outflow arrhythmias

Zhiyong Zhang[2], Xiaofeng Hou[1], Zhiyong Qian[1], Jianghong Guo[3], Jiangang Zou[1]

[1]Department of Cardiology, The First Affiliated Hospital of Nanjing Medical University, Nanjing 210029, Jiangsu, China; [2]Department of Cardiology, Suqian First People's Hospital, Suqian 223800, Jiangsu, China; [3]Department of Cardiology, Rugao First People's Hospital, Suqian 223800, Jiangsu, China

Received March 22, 2021; Accepted May 12, 2021; Epub August 15, 2021; Published August 30, 2021

Abstract: Objective: To explore the characteristics of optimal ablation site and its surrounding tissue in terms of unipolar and bipolar voltage mapping in idiopathic arrythmias from right ventricular outflow tract (RVOT) to understand if there is any difference between the two arrhythmias in matrix. Method: A total of 40 patients with idiopathic arrhythmias originated from RVOT (28 PVCs/12 VT) were enrolled in the study group. The control group consisted of five patients with supraventricular tachycardia (SVT). Before ablation, the CARTO system was applied to establish a detailed three-dimensional electroanatomic voltage map (EVM) of RVOT during the sinus rhythm. Results: A band-like LVA of similar size was observed under the pulmonary valve on not only the bipolar map, but also unipolar map, for every patient. Both unipolar and bipolar voltage values in areas within 5 mm were significantly different from those in other areas above ablation targets, whereas similar differences were observed only in unipolar voltage values below the optimal ablation site for either of the two arrhythmias. Significant difference was present between VT group and VPCs group in voltage values for every area including target site. In terms of the overall LVA areas and the scar areas displayed on the unipolar and bipolar voltage maps, there was a significant difference between the unipolar value and bipolar value for the LVA areas and the scar areas in the VT or PVC group ($P<0.05$). Conclusions: There was focal micro-scarring around the optimal ablation site. The ectopic focus is probably located in mid- or epimyocardium. The distributions of majority of optimal ablation sites were regular especially at the noteworthy border of the band-like LVA on bipolar voltage map, or in the band-like LVA on unipolar voltage map.

Keywords: Electroanatomic voltage mapp (EVM), right ventricular outflow tract (RVOT), ventricular tachycardia (VT), premature ventricular contractions (PVCs)

Introduction

The mechanism of idiopathic arrhythmias originated from right ventricular outflow tract (RVOT) is not fully understood currently. To date, few studies on the relationship between the two types of arrhythmias including premature ventricular contractions (PVCs) and ventricular tachycardia (VT) have been reported [1, 2]. In recent years, electroanatomic voltage mapping (EVM) has become a new and sensitive method for matrix research of arrhythmias to identify and characterize low-voltage regions and conduction. It is increasingly used for substrate-based mapping and catheter ablation of scar-related VT [3, 4]. It has been suggested that unipolar EVM provide a larger antenna than bipolar EVM to detect fibro-fatty subatrate involvement of epi- and mid-myocardium which is commonly present in ARVC patients [5-7]. In this study, we investigated the targets of IRVOA patients with different forms of arrhythmias and performed unipolar and bipolar voltage mapping around the target to characterize the similarities and differences between IRVOT PVC and VT matrixes, thus providing clinical guidance for the treatment of IRVOA.

Materials and methods

Patients

We recruited IRVOA patients and supraventricular tachycardia patients with successful ablation who were admitted to the Cardiovascular Medicine Department of Jiangsu Province Hos-

pital and Suqian First Hospital in China between January 2014 and September 2019. All included patients signed the informed consent form. The study was approved by the ethics committees of the respective hospitals (NCT-03895413).

Study group

Before the operation, ventricular arrhythmia patients with a preoperative electrocardiogram conforming to the origin characteristics of right ventricular outflow underwent cardiac ultrasound or coronary angiography and MRI to exclude ARVC and were clinically diagnosed as idiopathic PVC or VT [8, 9]. During the operation, all patients received detailed electrophysiological examination and radio-frequency ablation. The study group comprised the patients with successful ablation targets under the pulmonary valve. Pure PVC was defined as single PVC with the same form or continuous PVC ≤2 identified in electrocardiogram and dynamic electrocardiogram examinations; VT was defined as continuous PVC ≥3 recorded by electrocardiogram or dynamic electrocardiogram examination, and a tachycardia with a frequency >100 beats/min or single consistent form PVC. In total, 40 patients were enrolled in the study group (11 males and 29 females), with an average age of 42.38±13.90 years (18-69 years). Preoperative dynamic electrocardiogram examination showed that the total number of PVCs exceeded 6,000 beats/24 h, with an average premature contraction number of 31442.9± 20407.1 beats/24 h, and a premature contraction load of 25%±14%. Cardiac ultrasound using the Simpson method showed that the cardiac ejection fraction (EF) value was 63.88%±3.86%.

Control group

Patients with supraventricular tachycardia and radio-frequency ablation with no clinical history and no echocardiography to indicate organic heart disease were considered as the control group. The control group consisted of two male and three female patients, with an average age of 43.6±11.6 years.

All patients stopped using anti-arrhythmia drugs (Quinidine Sulfate Tablets, H11020970, China Resources Double-Crane Pharmaceutical Co., Ltd., 200 mg) for at least five half-lives before the operation and signed informed consent for electrophysiological study (EPS) and radiofrequency ablation procedure.

Methods

All patients were required to undergo a detailed electrophysiological examination to exclude those with left ventricular outflow origin, right ventricular outflow epicardial origin, and supravalvular pulmonary artery origin. Before ablation, EVM for RVOT during sinus rhythm was completed, including the supravalvular pulmonary artery portion and the near His bundle portion.

Electrophysiological examination: When the baseline of preoperative electrocardiogram monitoring showed spontaneous PVC or no spontaneous PVC, isoproterenol (Penglai Nuokang Pharmaceutical Co., Ltd., H37020549, batch number: 100166-201004, specification: 50 mg) was administered by intravenous drip (1-5 μg/min). In addition, electrocardiograms showing clinical PVC induced by routine procedures during the operation were further investigated. The Seldinger vascular puncturing method was used to puncture the right femoral vein and a 4-mm non-perfusion diagnostic/ablation deflectable tip catheter or a 3.5-mm perfusion diagnostic/ablation deflectable tip catheter (Navistar thermocool, biosense webster) was introduced to guide the voltage mapping during sinus rhythm and for activation mapping under PVC using the three-dimensional mapping CARTOXP system.

EVM: All patients underwent preoperative routine EVM for RVOT during sinus rhythm and sample collection (≥50 points) was performed between the supravalvular pulmonary artery portion and the near His bundle portion. We estimated the location of the pulmonary valve by the guidance of bi-axial fluoroscopy and right ventriculography. For the cases mapped by the CARTOXP system, the merged image of cardiac computer tomography and electrical mapping was used to confirm the location of the pulmonic valve. The bipolar frequency was 30-500 Hz, the unipolar frequency was 1-240 Hz, and the electrogram was generated at a speed of 200 m/s. The center of Wilson was used as the other pole in unipolar voltage mapping. The variation in the perimeter of recorded points was within 2%, the variation of local ventricular activation time was within 3 mm, and the varia-

Table 1. Baseline data of the patient in the PVC and VT groups in the study group

Group	Number	Sex (F/M)	Age (years)	LVEF (%)	Premature contraction load
VT group	12	10/2	45.0±10.5	64.6±4.0	27%±20%
PVC group	28	22/6	42.5±12.5	63.6±3.9	25%±10%
X^2/t		3.65	1.365	1.254	1.964
P-value (VT vs PVC)		0.227	0.538	0.436	0.649

Note: Data represent mean ± standard deviation. LVEF, left ventricular ejection fraction (Simpson method); premature contraction load, the ratio of the total number of individual PVCs to the total number of heartbeats in a 24-hour dynamic electrocardiogram. Electrophysiological examination and radio-frequency ablation. There were no significant differences in the ventricular rhythm data collected (81.1±51.1 points) between the PVC and VT groups (P=0.74). Ablation was successful in all the patients, and no arrhythmia appeared after half an hour or intravenous drug administration by drip.

tion of the local catheter location was within 4 mm. All these data were then integrated into images. In addition, the movement of the catheter was coordinated with the movement of the heart under fluoroscopy to determine whether the catheter and the heart were sufficiently abutted. In addition, different colors from the purple area (bipolar voltage ≥1.5 m or unipolar voltage ≥6 mV) to gray area (bipolar voltage <0.5 mV or unipolar voltage <3.5 mV) represented different regions from normal myocardium to the scar area, with the middle color representing the low voltage myocardium area according to previously reported criteria [10-12]. The distances from targets to the pulmonary valve on the bipolar voltage map of the study group were measured, and the unipolar and bipolar voltage values at optimal ablation sites were recorded. In addition, the LVA and scar area acreage on unipolar and bipolar voltage maps in the study group were measured, and the acreage of band-like LVA above the pulmonary valve in the study and control groups were measured, thus comparing the indexes in the study groups (the PVC group, the VT group) and the control group.

Radio-frequency ablation: The site of PVC or VT onset was determined by activation or pace mapping, and the ablation target was identified as the location of earliest local activation during arrhythmia or the amplitude of surface ECG with pace mapping displayed on at least 11 leads, consistent with that of spontaneous arrhythmia ECG. Ablation with the 4-mm catheter was carried out at 50-60°C, with a maximum power of 50 W and ablation time of 60-120 s. Ablation with the 3.5-mm head-end perfusion saline catheter was carried out at 42°C, with a maximum power of 50 W and ablation time of 60-120 s. When the routine procedure stimulation or intravenous drip of isoproterenol did not induce clinical PVC or VT, and no recurrence was observed after 30 min, it was regarded as a successful acute ablation, and was defined as the true target of the arrhythmia. According to the anatomy of the right ventricular outflow, the locations of targets were divided into ventricular septum (front, middle, rear) and free walls (front, middle, rear).

Statistical analysis

All data were analyzed using SPSS16.0 statistical software. The measurement data were expressed as mean ± standard deviation (SD), and *t*-test was adopted for comparisons between two samples. Count data were expressed as rate, and comparisons between two samples were analyzed by chi-square test or Fisher exact probability test. $P<0.05$ was considered to indicate statistically significant difference.

Results

Baseline

As shown in **Table 1**, there were no significant differences in the baseline data of the patients in the PVC and VT groups in the study group in terms of sex, age, LVEF, and premature contraction load ($P>0.05$).

Location distribution of targets

As shown in **Table 2**, 75% of patients had successful ablation targets located in the ventricular septum (30 of 40 cases), while 25% had targets in the free wall (10 of 40 cases). There was no significant difference between the VT and PVC group in the target distribution in ventricular septum or free wall ($P>0.05$).

The average distance of the targets from the pulmonary valve was 19.8±10.9 mm, among which, the distance was 19.2±8.9 mm in the

Table 2. Target location distribution in the PVC and VT groups

Target location	PVC group	VT group	χ^2	*P*-value (VT vs PVC)
Ventricular septum			4.369	0.896
Front	11	5		
Middle	4	3		
Rear	6	1		
Free wall				
Front	6	2		
Middle	0	0		
Rear	1	1		

Note: *P*>0.05. There was no significant difference in the distribution of target location (septum and free wall of RVOT) between the PVC and VT groups.

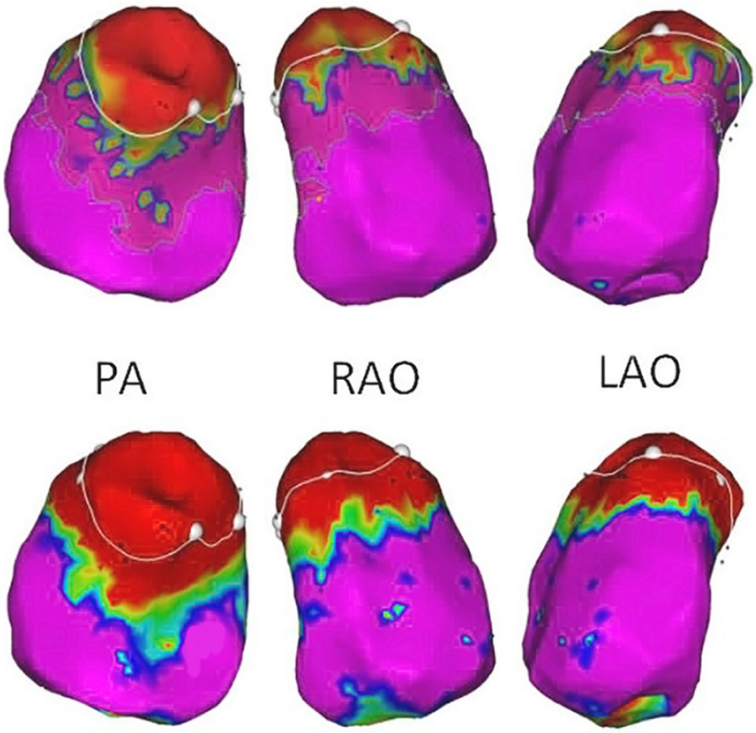

Figure 1. Right ventricular outflow unipolar and bipolar EVM under different planes (PA, RAO, LAO) in the control group.

PVC group, and 21.4±14.9 mm in the VT group, with no significant difference between the two groups (*P*>0.05).

EVM of the control group

The unipolar and bipolar voltage maps showed similar band-like LVAs under the pulmonary valve in different planes. Specifically, the areas of the pulmonary valve and band-like LVAs displayed in the unipolar voltage map were significantly lower and wider than those in the bipolar voltage map (*P*<0.05). Unipolar and bipolar EVM of right ventricular outflow under different planes (PA, RAO, LAO) in the control group was shown in **Figure 1**.

EVM of the study groups (PVC and VT groups)

In the study group, an average of 106±60.1 points were collected during the sinus rhythm, with no significant difference between the PVC and VT groups (*P*=0.57). In the study group, the unipolar voltage value at targets was 9.90±4.71 mV and bipolar voltage value was 3.27±2.71 mV. As shown in **Table 3**, there was no significant difference in unipolar and bipolar values between the PVC and VT groups (*P*>0.05), although there were significant differences between unipolar voltage value and the bipolar voltage value within the groups (*P*<0.05).

Relationship between targets and the location of band-like LVAs under the pulmonic valve in the study group

Both unipolar and bipolar maps displayed a similar band-like LVA under the pulmonary valve for every patient. Relationships between target and the band-like LVA on both unipolar and bipolar voltage map of a VPCS patient in different views (PA: Postero-anterior; RL: Right lateral; and LL: Left lateral) are shown in **Figure 2** and **Table 4** (The blue dot denotes the target, which is at the border of the LVA on bipolar voltage map and in the LVA on unipolar map). Relationships between target and the band-like LVA on both unipolar and bipolar voltage map of a VT patient in different views (PA: Postero-anterior; RL: Right lateral; and LL: Left lateral) are shown in **Figure 3** (The blue dot denotes the target, which is at the border of the LVA on bipolar voltage map and in

Table 3. Comparison of voltage data at targets between the PVC and VT groups

	Voltage at PVC targets (mV)	Voltage at VT targets (mV)	*t*	*P*-value (VT vs PVC)
Unipolar voltage map	9.79±5.20	10.14±3.47	1.374	*0.486*
Bipolar voltage map	2.86±2.05	3.96±2.46	1.569	0.523
t	*2.654*	*2.987*		
P-value (Unipolar VS Bipolar)	*0.001*	*0.001*		

Note: The difference between the unipolar voltage value and bipolar voltage value at targets within the groups was statistically significant (P<0.001). The difference in both the unipolar and bipolar voltage values between the PVC and VT at targets was not statistically significant (P>0.05).

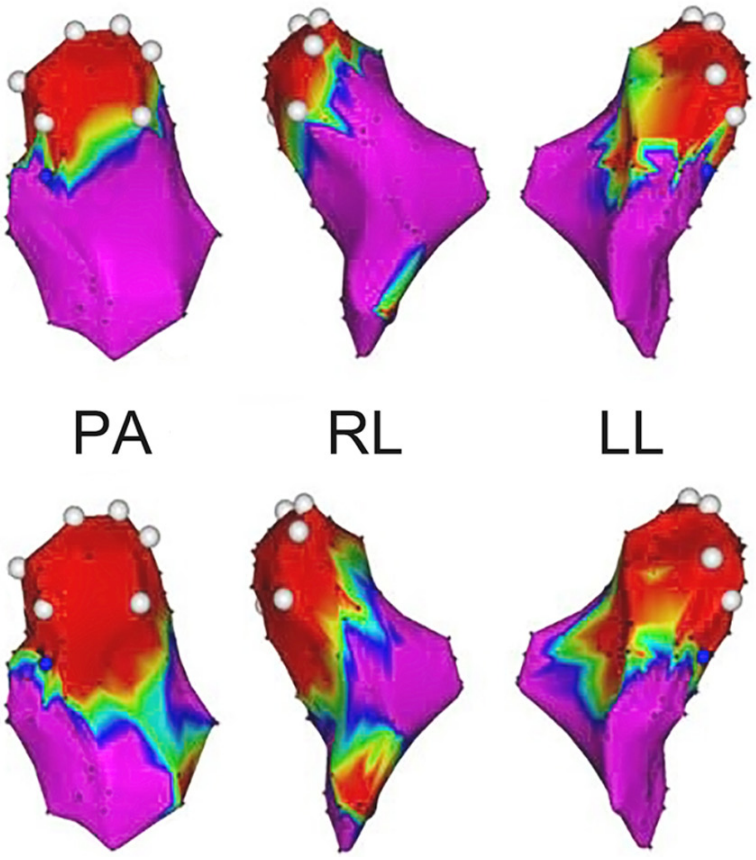

Figure 2. Relationship between target and the band-like LVA on both unipolar and bipolar voltage map of a VPCS patient in different views (PA: Postero-anterior; RL: Right lateral; and LL: Left lateral). The blue dot denotes the target, which is at the border of the LVA on bipolar voltage map and in the LVA on unipolar map.

the LVA on unipolar map). Specifically, there was no significant difference in the band-like LVAs area under pulmonic valve among the control, VT and PVC groups (*P*>0.05), as shown in **Table 5**.

On the bipolar map, the targets for 22.5% (9/40 cases) patients located in the band-like LVA under the pulmonic valve, for 47.5% (19/40 cases) patients at the border of the band-like LVA, and 30.0% (12/40 cases) patients below the band-like LVA border (in the normal area).

But on the unipolar map, the targets for 47.5% (19/40 cases) patients located in the band-like LVA, 40% (16/40 cases) at the border of the band-like LVA, and 12.5% (5/40 cases) outside the band-like LVA (2 patients below the band-like LVA border, 3 patients above the band-like LVA in the scar area). There was no significant difference in target distribution between VPCs and VT group on the bipolar or unipolar map. But there was significant difference in target distribution between the unipolar and bipolar voltage maps only for VPCs group, but not for VT group, as shown in **Table 5**. There were significant differences in the amplitude index and time limit index of the R wave in lead V2, and the R wave transition zone in the ECG axis and chest leads (**Figure 4**).

EVM of myocardial tissues in the vicinity of targets

The RAO posture was selected, and the EVM in areas of 0-5 mm, 5-10 mm, and 10-15 mm around the targets were compared. Schematic

Table 4. Comparison of unipolar and bipolar voltage map areas of the band-like LVAs under pulmonary valve among the three groups (cm^2)

Band-like LVA area	Control group	PVC group	VT group	F	*P*-value (Uni vs Bi)
Unipolar voltage map	7.02±2.53	11.06±6.05	11.34±3.69	45.964	0.001
Bipolar voltage map	4.22±1.34	6.52±3.07	4.97±4.00	56.389	*0.001*
t	2.677	5.369	4.634		
P-value (control vs study group)	*0.161*	*0.136*	*0.524*		

Note: The difference in the band-like LVAs area between the unipolar and bipolar voltage map among the three groups was statistically significant (P<0.001). The difference in the band-like LVAs area among the three groups on the bipolar or unipolar map was not statistically significant (P>0.05).

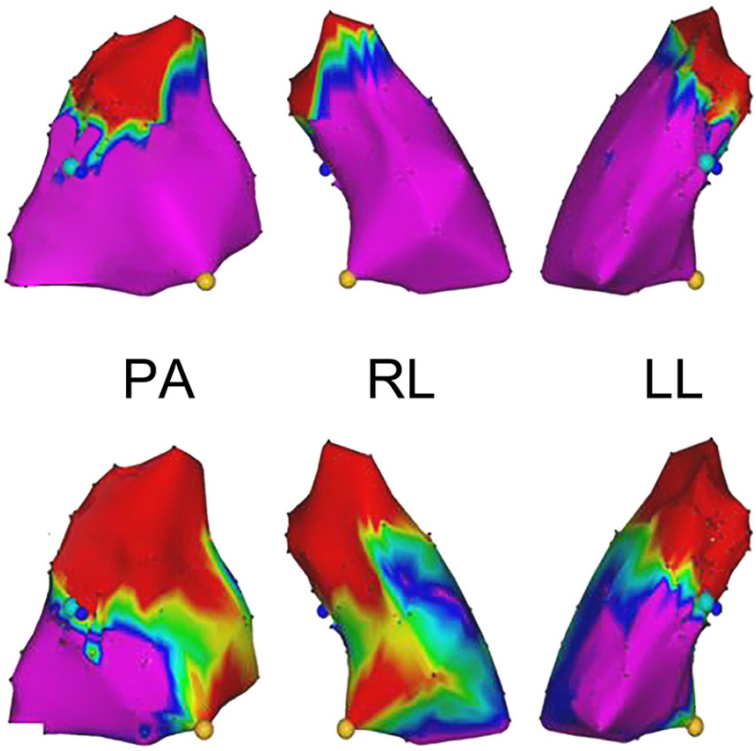

Figure 3. Relationship between target and the band-like LVA on both unipolar and bipolar voltage maps of a VT patient in different views (PA: Postero-anterior; RL: Right lateral; and LL: Left lateral). The blue dot denotes the target, which is at the border of the LVA on bipolar voltage map and in the LVA on unipolar map.

diagrams of different areas of targets under unipolar and bipolar voltage mapping are shown in **Figure 5**.

The unipolar voltage value in the area 0-5 mm above the targets was significantly different from those in the areas 5-10 mm and 10-15 mm above the targets (*P*<0.05), while the unipolar voltage value in the area 5-10 mm above the targets was not significantly different from that in the area 10-15 mm above the targets (*P*>0.05). The bipolar voltage maps followed a similar pattern.

The unipolar voltage value in the area 0-5 mm below the targets was significantly different from those in the areas 5-10 mm and 10-15 mm below the targets (*P*<0.05), while the unipolar voltage value in the area 5-10 mm below the targets was not significantly different from that in the area 10-15 mm below the targets (*P*>0.05). In addition, there were no significant differences among the voltage values in the three areas on the bipolar voltage map (*P*>0.05).

Comparison of the unipolar and bipolar voltage values of different areas around the targets between the PVC and VT groups is shown in **Table 6**.

Overall areas of LVA and scar area in the voltage map of the study group

In terms of the overall LVA areas displayed in the unipolar and bipolar voltage maps, there was no significant difference between the PVC and VT groups (*P*>0.05), while there was a significant difference between the unipolar and bipolar voltage maps in the VT and PVC groups (*P*<0.05). A similar pattern was observed in the scar area. The overall LVAs in the study group are shown in **Table 7**, while the overall scar area is shown in **Table 8**.

Discussion

In this study, we explored the characteristics of optimal ablation sites and their surrounding tissues in terms of unipolar and bipolar voltage

Table 5. Relationship between the targets and the band-like LVA under the pulmonic valve

	Location	Within LVA	Border of the LVA	Outside LVA	VE vs VT Target distribution	
Bipolar EVM	PVC group targets	6	12	10	χ^2=1.655	*P=0475* (*in bipolar EVM*)
	VT group targets	3	7	2		
Unipolar EVM	PVC group targets	15	10	3	χ^2=5.369	P=0.499 (in unipolar EVM)
	VT group targets	4	6	2		

Note: Unipolar EVM vs bipolar EVM PVCs group VT group in targets distribution. χ^2=5.789, P=0.020; Target distribution χ^2=4.559, P=0.896.

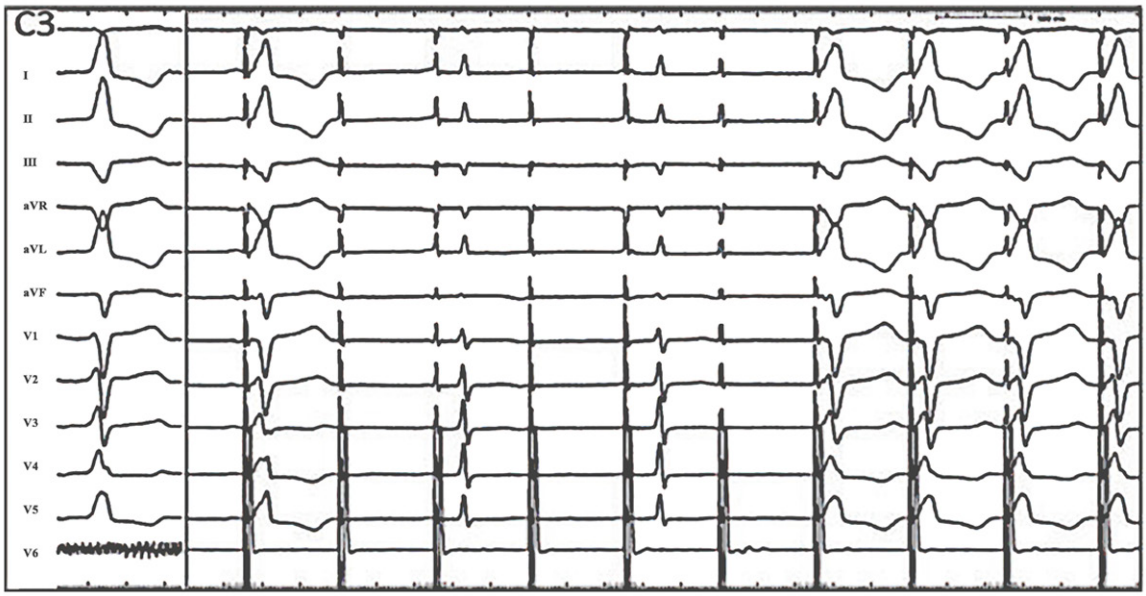

Figure 4. 12-lead ECG pace maps.

mapping in idiopathic arrythmias from RVOT to understand if there is any difference between the two arrhythmias (VPCs and VT) in matrix. The main results of the study include that the matrix of the two types of arrhythmia from RVOT appeared alike; there was focal microscarring around the optimal ablation site. The ectopic focus may be located in mid- or epimyocardium. The distributions of majority of optimal ablation sites were regular to some extent, especially the noteworthy border of the band-like LVA on bipolar voltage map or in the band-like LVA on unipolar voltage map. The addition of EVM to intracardiac electrophysiological study provided significant added value for successful ablation.

Location of successful ablation targets

In this study, we showed for the first time that there were no significant differences in the areas of the band-like LVAs under the pulmonary valves in the three groups, indicating that LVA is caused by a common anatomical structure. During the development of the heart in human embryo, part of the myocardium in the distal outflow tract degenerates and evolves into the ascending aorta or pulmonary artery trunk. In addition, partially degenerated RVOT myocardial tissues may form residual myocardial sleeves, which can reach 3-6 mm in thickness, and extend to any height in the valve, even reaching the supravalvular pulmonary artery and connecting the right ventricular myocardium and pulmonary valve. However, the lack of homogeneity in the electrophysiological characteristics of the incompletely degenerated cardiomyocytes and surrounding normal myocardium cells may induce related arrhythmia [11, 12]. Additionally, the band-like LVA under the pulmonary valve in the control and study groups faced this part, showing lower

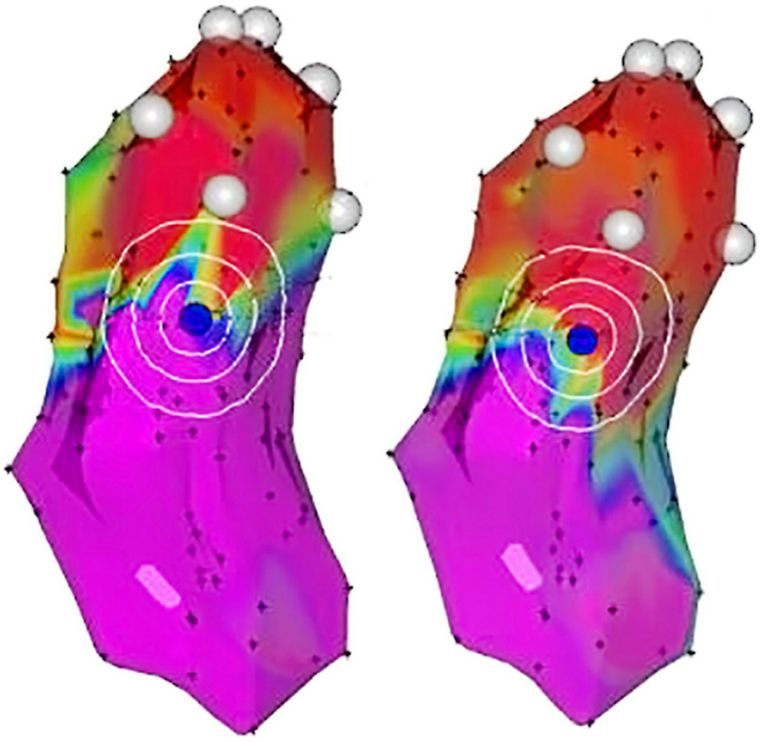

Figure 5. Schematic diagram of different areas of targets under unipolar and bipolar voltage mapping.

edge gaps and band-like protrusions, connecting the RVOT and the pulmonary valve, which may represent the area of the myocardial sleeve. The area displayed in unipolar voltage mapping was significantly larger than that in the bipolar voltage map, suggesting that there is a large transition area under the intima near the right ventricular outflow pulmonary valve, which is an area of low voltage, and consistent with the actual anatomical structure.

In accordance with the results of our study, previous research using traditional two-dimensional X-ray and three-dimensional electrophysiology anatomy mapping systems suggested that targets tend to occur on the side of the RVOT septum, below the pulmonary valve [12, 13], or the transition area between the outflow tract and the pulmonary valve [14]. Specifically, among the 40 patients in the study group, 75% of the targets were distributed in the ventricular septum. There was no significant difference between the PVC and VT group targets in terms of the target distribution in the ventricular septum and free wall. In addition, most patients with ventricular septum targets were anterior (53%, 16 of 30 cases), and most patients with free wall targets were anterior (80%, 8 of 10 cases), which is consistent with the results reported by Yu et al. [15]. Specifically, there were more patients with subvalvular targets than those with supravalvular targets, and the majority of supravalvular were left sinus, which may not be consistent with the criteria for defining the pulmonary valve.

The analysis of relationship between the targets and the band-like LVA under the pulmonary valve showed that the voltage transition zone (band-like LVA) under the pulmonary valve, especially the LVA border, is the site where the VA originating from the RVOT easily occurs. On the bipolar map, the targets for 22.5% (9/40 cases) patients located in the band-like LVA under the pulmonic valve, for 47.5% (19/40 cases) patients at the border of the band-like LVA, and for 30.0% (12/40 cases) patients below the band-like LVA border (in the normal area). But on the unipolar map, the targets for 47.5% (19/40 cases) patients located in the band-like LVA, 40% (16/40 cases) at the border of the band-like LVA, and 12.5% (5/40 cases) outside the band-like LVA (2 patients below the band-like LVA border, 3 patients above the band-like LVA in the scar area). There was no significant difference in target distribution between VPCs and VT group on the bipolar or unipolar map. However, there was significant difference in target distribution between the unipolar and bipolar voltage maps only for VPCs group, but not for VT group, which is consistent with the results of previous studies at home and abroad. Furushima et al. [16, 17] and Yamashi et al. [18] found that the origin or exit of RVOT arrhythmia was located predominantly at the voltage junction and the edge of LVA. Wang et al. [19] showed that 91.7% of ablation targets were in the voltage transition zone of the pulmonary valve, 2.0% were in the LVA under the pulmonary valve, and 6.7% of the local voltage of the ablation targets was normal. Lin et al. [20] found that 67% of the targets were in the transi-

Table 6. Comparison of the unipolar and bipolar voltage values of different areas around the targets between the PVC and VT groups (Data represent the mean ± standard deviation)

Group	Location (targets above or below, mm)	PVC group voltage (mV)	VT group voltage (mV)	t	*P*-value
Unipolar	0-5 mm above	4.52±2.41	4.94±1.90	1.894	0.001#
	5-10 mm above	3.34±1.69	3.37±1.95	5.689	0.001*
	10-15 mm above	3.02±2.04	3.64±2.21	6.597	0.999¥
	F=5.987	P=0.582[a]			0.001[c]
	0-5 mm below	5.39±2.67	5.65±2.30	6.358	0.001#
	5-10 mm below	6.38±2.67	7.81±2.85	7.645	0.002*
	10-15 mm below	7.25±3.11	7.85±4.79	1.324	0.999¥
	F=9.674	P=0.385[b]			0.001[c]
Bipolar	0-5 mm above	1.68±1.78	2.03±2.54	7.546	0.006#
	5-10 mm above	1.35±1.64	0.77±0.77	8.654	0.006*
	10-15 mm above	0.84±1.23	0.94±1.06	9.687	0.999¥
	F=7.978	P=0.923[a]			0.001[c]
	0-5 mm below	3.18±1.99	3.05±3.11	1.325	0.999#
	5-10 mm below	3.42±1.55	3.49±2.69	1.645	0.999*
	10-15 mm below	3.91±2.08	3.09±1.83	1.756	0.999¥
	F=5.478	P=0.593[b]			0.555[c]

Note: #comparison of the 0-5 mm radius above the target and 5-10 mm radius above the target, and comparison of the 0-5 mm radius below the target and 5-10 mm radius below the target; *comparison of the 0-5 mm radius above the target and 10-15 mm radius above the target, and comparison of the 0-5 mm radius below the target and 10-15 mm radius below the target; ¥comparison of the 5-10 mm radius above the target and 10-15 mm radius above the target, and comparison of 5-10 mm radius below the target and 10-15 mm below the target. [a]comparison of the voltages in the three areas (0-5 mm, 5-10 mm, 10-15 mm radius) above target between the PVC and VT groups; [b]comparison of the voltages in the three areas (0-5 mm, 5-10 mm, 10-15 mm radius) below target between the PVC and VT groups; [c]comparison of the voltages in the three areas (0-5 mm, 5-10 mm, 10-15 mm radius) above and below target between the PVC and VT groups.

Table 7. Comparison of the overall LVA between the PVC and VT groups (cm^2)

	PVC group LVA area	VT group LVA area	Area difference, *P* (Uni vs Bi)
Unipolar voltage map	15.16±9.20	13.94±6.17	5.228 (*P*=0.001)
Bipolar voltage map	8.42±3.43	10.23±8.75	95% CI: 2.157, 8.299
Area difference (PVC vs VT group)	0.296 (*P*=0.879) (95% CI: -3.625, 4.217)		

Note: The difference in LVA areas between unipolar and bipolar voltage maps for either of arrhythmias was statistically significant at 5.228 (P=0.001) (95% CI: 2.157, 8.299). The difference in LVA areas between PVC and VT groups on unipolar voltage map or bipolar voltage map was not statistically significant at 0.296 (P=0.879) (95% CI: -3.625, 4.217).

Table 8. Comparison of overall scar areas in the PVC and VT groups (cm^2)

	PVC group scar area	VT group scar area	Difference *P* (Uni vs Bi)
Unipolar voltage map	17.60±10.23	14.59±12.18	7.060 (P=0.001)
Bipolar voltage map	10.07±7.88	8.00±5.50	95% CI: 3.449, 10.671
Area difference (PVC vs VT group)	2.540 (P=0.341) (95% CI: -2.796, 7.876)		

Note: The difference in the scar area between unipolar and bipolar voltages map for either of arrhythmias was statistically significant at 2.540, 7.060 (P=0.001) (95% CI: 3.449, 10.671). The difference in the scar area between PVC and VT groups on unipolar voltage map or bipolar voltage map was not statistically significant at 2.540 (P=0.341) (95% CI: -2.796, 7.876).

tion area in the VT group, which had more targets than the PVC group due to the difference in the origin of LVAs. These findings are in conflict with the results of our study, but may be related to the inconsistency of the relevant transition zone concept. Liu et al. [21] showed that isolated diastolic potentials (IDPs) were recorded at the origin region in right ventricular outflow ventricular arrhythmia patients, and the successful ablation targets were located in

the IDP area or at the edge. It is thought that the voltage junction area may be composed of normal myocardial tissue, fibrous tissue or primary myocardium and injured myocardium, leading to heterogeneous conduction in electrocardiograms. This concept validates our conclusions from another perspective. In addition, the distribution of targets on the bipolar voltage map during sinus rhythm mapping seems to be similar to that on the unipolar voltage map. If the bipolar voltage map is distributed in the normal area, the unipolar voltage map shows that the targets are mostly in unipolar LVA or LVA edge. If the bipolar voltage map is in LVA, the unipolar voltage map may be in the scar area. In conclusion, our findings suggest the existence of matrix differences between the superficial layer and deep layers of the right ventricular outflow wall.

Analysis of voltage at targets and its surrounding voltage mapping

In this study, there was no significant difference in the voltage values of targets in the unipolar and bipolar maps between the PVC and the VT groups. However, further comparisons of the voltage maps revealed that there was a significant difference in the voltage values between the areas located 0-5 mm, 5-10 mm and 10-15 mm around the targets in the bipolar mapping. In addition, the average voltage within the range of 0-5 mm above the target was normal, indicating the existence of obvious matrix changes outside the area 5 mm above the targets, as well as low voltage and areas of scarring. There was little change in the matrix in different regions 5-15 mm below the bipolar voltage map targets. In contrast, the unipolar voltage map showed that the area 0-5 mm above the targets was LVA, while scarring occurred beyond the 5-mm areas, with obvious matrix changes. Because the unipolar voltage map reflects deeper myocardial scars, the focal point is in the deep region. Additionally, there were micro-scars in the region 5 mm around the focal point, which differed significantly from the matrix in the area beyond 5 mm. This is consistent with the experimental model showing that the presence of a non-excitable conduction damage zone around the pacemaker is a prerequisite of premature contraction, ventricular parasystole and activation of VT of the outflow tract. Nevertheless, this result was not found in previous studies. It was clear that there was focal micro-scarring around the ectopic beats of the right ventricular outflow ventricular arrhythmia. There was no significant difference in the unipolar and bipolar mapping in the different areas near the targets in the VT and PVC groups, suggesting that the matrixes in the VT and PVC groups are similar. In addition, the LVA and the total scar area in the right ventricular outflow constructed in VT and PVC patients were analyzed. The results showed that the area on the unipolar voltage map was significantly greater than that on the bipolar voltage map, and there was no difference in the LVA area or the total scar area on the unipolar and bipolar voltage maps between the PVC group and VT group, further supporting the role of focal micro-scarring in the mechanism supporting their occurrence. At the same time, the above comparisons showed that the unipolar voltage map is superior to the bipolar voltage map in reflecting the depth and breadth of the scars.

All successful RVOT PVC ablation targets in this study were located under the anatomic pulmonary valve. The distance between the target and the anatomic pulmonary valve was 19.8± 10.9 mm, with the nearest distance approximately 4 mm and no significant difference between the PVC and the VT groups. However, the conventional catheter operation method (non-inverted U-shape) has been adopted in many studies, including our own, and the pulmonary valve mapping ablation effectively supports the ablation targets of abnormal voltage regions under the pulmonary valve, which may be the origin of PVC. Nevertheless, because the valve was not crossed before ablation, and the inverted U was used to routinely map the area of the intrapulmonary sinus, it cannot be ruled out that this is not the only outlet for PVC transmission. Liao et al. [28] found that pulmonary sinus ablation successfully resolved many cases of failure or recurrence of ablation during the PVC, suggesting that the pulmonary sinus is also one of the origins of RVOT PVC. Subsequently, Yang et al. [29] studied the PVC of the origin of the left pulmonary sinus by using conventional non-inverted U catheters to accomplish ablation. Zhang et al. [30] routinely used inverted U-shape catheter behind the transpulmonary valve to successfully ablate 96.3% of RVOT VA patients in the pulmonary sinus, thus providing challenges for conventional subvalvular ablation. Notably, in early clinical

studies of RVOT PVC ablation, a success rate of almost 90% was also achieved using traditional mapping and ablation strategies. Targets were successfully ablated under the valve using traditional non-inverted U-shaped catheters, including some targets that were distant from the LVA, so the argument that the use of subvalvular ablation targets is just the outlet of activation cannot be supported. In this study, we found that the actual anatomic location of the pulmonary sinus was lower than that of the pulmonary valve, and the ablation targets of some lower sinuses were even closer to the tricuspid annulus. The abnormal region of the pulmonary valve voltage measured using the traditional mapping method can extend to the portion of the pulmonary valve, but was higher in the anatomical location than the so-called "supervallar" region in the pulmonary sinus. Moreover, this part of the voltage abnormal area also includes the corresponding subvalvular area in the pulmonary sinus. Therefore, although the pulmonary sinus is regarded as supervallar anatomical structure, if the level of the pulmonary annulus is taken as the dividing line, the pulmonary sinus and the area of abnormal subvalvular voltage in the traditional sense are located at the same level anatomically and are adjacent to each other. Hence, the particular characteristics of this anatomical structure cause some difficulties in determining the origin of PVC. Gami et al. [31] found that myocardial sleeve tissues near the pulmonary valve were present in 74% of the subjects without VA. Additionally, myocardial sleeve tissues were commonly found above the pulmonary sinuses and between the sinuses, but occurred at much lower frequency (1.7%) in the sinuses. However, using a combination of three-dimensional mapping and intracardiac echocardiography, Liu et al. [32] found that about half of the RVOT PVC originated above the pulmonary valve (6-10 mm from the valve). In conclusion, despite differences in the anatomical structure of the pulmonary sinus, supravalvular pulmonary artery and subvalvular pulmonary artery, these structures are actually located in the abnormal voltage region in three-dimensional voltage mapping, which is consistent with the conclusions of this study. Regardless of the use of the new inverted U-shaped catheter operation method or the traditional catheter mapping strategy, in fact, the myocardial sleeve distribution area (the so-called abnormal voltage area) near the pulmonary valve cannot be completely covered. For example, patients in this study with targets below the LVA also had a high proportion of abnormal voltage areas. There were two cases close to the anatomic pulmonary valve in the LVA, which did not fully support the explanation of the ablation point as the outlet. However, intra-sinus ablation is also a stable catheter operation method that is carried out near the targets, especially the so-called focal origin of the LVA above the sinus floor.

Limitations

As the location of the pulmonary valve cannot be identified by a specific mark, and there is no clear definition of the annulus, the combination of X-ray and potential characteristics is usually adopted for preliminarily judgments. Therefore, the critical point of the intraluminal bipolar voltage map was used as the location of the pulmonary valve annulus. Indeed, the interface between the scar area and the low voltage on the electroanatomic mapping was used as the lower boundary of the pulmonary valve annulus in the electrical sense, thereby providing an anatomical relationship between the sinus floor, annulus, and electrical annulus. On the other hand, LVA is the transition area during the pulmonary valve annulus. Because the right ventricular outflow appears as a tubular structure, the LVA below the pulmonary valve annulus also appears as an irregular, ring-shaped structure; thus, it is impossible to measure its actual width. Moreover, because there were not enough patients with successful sinus ablation, further studies should be performed later. The selected patients were diagnosed by ultrasound and electrocardiogram imaging, and high-risk patients were examined by coronary contrast CT (CTA) and other clinical examinations to rule out common ischemic and non-ischemic heart disease. For patients with a large RVOT LVA distribution, no cardiac MRI was performed, so ARVC and sarcoidosis could not be ruled out.

Conclusions

In this study, based on the analysis of the characteristics of IRVOT targets and the comparison of unipolar and bipolar voltage maps in different ranges around the targets, we further confirmed that similar band-like LVAs exist below the pulmonary valve of IRVOA patients

and supraventricular tachycardia patients in the control group. In addition, the band-like LVAs, especially the band-like LVA border, is the position most prone to VA of RVOT origin. In addition, both the unipolar and bipolar voltage maps showed that LVA exists within a certain range around the targets in the VT and PVC group, and the unipolar voltage map provides greater clarity than bipolar voltage map. Hence, it can be inferred that focal micro-scarring occurs around the right ventricular outflow ventricular arrhythmia. More importantly, the local matrixes of the VT and PVC are the same. Specially, the unipolar electrogram is superior to the bipolar electrogram in terms of the LVA and area and depth of scar area. The distribution characteristics contribute to identification of intraoperative targets. Notably, supravalvular pulmonary artery sinus in patients with targets that are difficult to ablate is not a trivial issue, and the results can be unexpected.

Disclosure of conflict of interest

None.

Address correspondence to: Jiangang Zou, Department of Cardiology, The First Affiliated Hospital of Nanjing Medical University, 300 Guangzhou Road, Nanjing 210029, China. Tel: +86-025-83714511; E-mail: zoujgnj@163.com

References

[1] Gard JJ and Asirvatham SJ. Outflow tract ventricular tachycardia. Tex Heart Inst J 2012; 39: 526-528.

[2] Klein LS, Shih HT, Hackett FK, Zipes DP and Miles WM. Radiofrequency catheter ablation of ventricular tachycardia in patients without structural heart disease. Circulation 1992; 85: 1666-1674.

[3] Zhong L, Lee YH, Huang XM, Asirvatham SJ, Shen WK, Friedman PA, Hodge DO, Slusser JP, Song ZY, Packer DL and Cha YM. Relative efficacy of catheter ablation vs antiarrhythmic drugs in treating premature ventricular contractions: a single-center retrospective study. Heart Rhythm 2014; 11: 187-193.

[4] Takemoto M, Yoshimura H, Ohba Y, Matsumoto Y, Yamamoto U, Mohri M, Yamamoto H and Origuchi H. Radiofrequency catheter ablation of premature ventricular complexes from right ventricular outflow tract improves left ventricular dilation and clinical status in patients without structural heart disease. J Am Coll Cardiol 2005; 45: 1259-1265.

[5] Lin T, Conti S, Cipolletta L, Marino V, Zucchetti M, Russo E, Pizzamiglio F, AlMohani G, Pala S, Catto V, Biase LD, Natale A, Tondo C and Carbucicchio C. Right ventricular outflow tract arrhythmias: benign or early stage arrhythmogenic right ventricular cardiomyopathy/dysplasia? J Atr Fibrillation 2014; 7: 1161.

[6] Gaita F, Giustetto C, Di Donna P, Richiardi E, Libero L, Brusin MC, Molinari G and Trevi G. Long-term follow-up of right ventricular monomorphic extrasystoles. J Am Coll Cardiol 2001; 38: 364-370.

[7] Tsai CF, Chen SA, Tai CT, Chiang CE, Lee SH, Wen ZC, Huang JL, Ding YA and Chang MS. Idiopathic monomorphic ventricular tachycardia: clinical outcome, electrophysiologic characteristics and long-term results of catheter ablation. Int J Cardiol 1997; 62: 143-150.

[8] Corrado D, Basso C, Leoni L, Tokajuk B, Turrini P, Bauce B, Migliore F, Pavei A, Tarantini G, Napodano M, Ramondo A, Buja G, Iliceto S and Thiene G. Three-dimensional electroanatomical voltage mapping and histologic evaluation of myocardial substrate in right ventricular outflow tract tachycardia. J Am Coll Cardiol 2008; 51: 731-739.

[9] Boulos M, Lashevsky I and Gepstein L. Usefulness of electroanatomical mapping to differentiate between right ventricular outflow tract tachycardia and arrhythmogenic right ventricular dysplasia. Am J Cardiol 2005; 95: 935-940.

[10] Polin GM, Haqqani H, Tzou W, Hutchinson MD, Garcia FC, Callans DJ, Zado ES and Marchlinski FE. Endocardial unipolar voltage mapping to identify epicardial substrate in arrhythmogenic right ventricular cardiomyopathy/dysplasia. Heart Rhythm 2011; 8: 76-83.

[11] Campos B, Jauregui ME, Park KM, Mountantonakis SE, Gerstenfeld EP, Haqqani H, Garcia FC, Hutchinson MD, Callans DJ, Dixit S, Lin D, Riley MP, Tzou W, Cooper JM, Bala R, Zado ES and Marchlinski FE. New unipolar electrogram criteria to identify irreversibility of nonischemic left ventricular cardiomyopathy. J Am Coll Cardiol 2012; 60: 2194-2204.

[12] Migliore F, Zorzi A, Silvano M, Bevilacqua M, Leoni L, Marra MP, Elmaghawry M, Brugnaro L, Dal Lin C, Bauce B, Rigato I, Tarantini G, Basso C, Buja G, Thiene G, Iliceto S and Corrado D. Prognostic value of endocardial voltage mapping in patients with arrhythmogenic right ventricular cardiomyopathy/dysplasia. Circ Arrhythm Electrophysiol 2013; 6: 167-176.

[13] De Ponti R and Ho SY. Mapping of right ventricular outflow tract tachycardia/ectopies: activation mapping velsus pace mapping. Heart Rhythm 2008; 5: 345-347.

[14] Hasdemir C, Aktas S, Govsa F, Aktas EO, Kocak A, Bozkaya YT, Demirbas MI, Ulucan C, Ozdogan O, Kayikcioglu M, Can LH and Payzin S. Demonstration of ventricular myocardial extensions into the pulmonary artery and aorta beyond the ventriculo-arterial junction. Pacing Clin Electrophysiol 2007; 30: 534-539.

[15] Corrado D, Basso C, Leoni L, Tokajuk B, Bauce B, Frigo G, Tarantini G, Napodano M, Turrini P, Ramondo A, Daliento L, Nava A, Buja G, Iliceto S and Thiene G. Three-dimensional electroanatomic voltage mapping increases accuracy of diagnosing arrhythmogenic right ventricular cardiomyopathy/dysplasia. Circulation 2005; 111: 3042-3050.

[16] Verma A, Kilicaslan F, Schweikert RA, Tomassoni G, Rossillo A, Marrouche NF, Ozduran V, Wazni OM, Elayi SC, Saenz LC, Minor S, Cummings JE, Burkhardt JD, Hao S, Beheiry S, Tchou PJ and Natale A. Short- and long-term success of substrate-based mapping and ablation of ventricular tachycardia in arrhythmogenic right ventricular dysplasia. Circulation 2005; 111: 3209-3216.

[17] Yamashina Y, Yagi T, Namekawa A, Ishida A, Sato H, Nakagawa T, Sakuramoto M, Sato E and Yambe T. Distribution of successful ablation sites of idiopathic right ventricular outflow tract tachycardia. Pacing Clin Electrophysiol 2009; 32: 727-733.

[18] Bogun F, Taj M, Ting M, Kim HM, Reich S, Good E, Jongnarangsin K, Chugh A, Pelosi F, Oral H and Morady F. Spatial resolution of pace mapping of idiopathic ventricular tachycardia/ectopy originating in the right ventricular outflow tract. Heart Rhythm 2008; 5: 339-344.

[19] Wang J, Liu XY and Chu JM. Relationship between ablation sites of idiopathic right ventricular outflow tract arrhythmia and endocardial voltage mapping. Chin Circulation J 2013; 28 : 199-202.

[20] Lin YZ, Chen L and Yang ZP. Electrophysiological characteristics of earliest activation in ventricular arrythmias originating from right ventricular outflow tract, correlation with voltage mapping. Chin J Cardiac Arrhyth 2016; 20: 21-25.

[21] Liu XY, Zhao YJ and Wang LX. The significance of isolated diastolic potentials in origin regions of idiopathic right ventricular outflow tract ventricular arrhythmias. Chin J Cardiac Pacing Electrophysiol 2013; 27: 294-299.

[22] van Huls van Taxis CF, Wijnmaalen AP, den Uijl DW, Gawrysiak M, Putter H, Schalij MJ and Zeppenfeld K. Reversed polarity of bipolar electrograms to predict a successful ablation site in focal idiopathic right ventricular outflow tract arrhythmias. Heart Rhythm 2011; 8: 665-671.

[23] Fisher WG, Bacon ME and Swartz JF. Use of an orthogonal electrode array to identify the successful ablation site in right ventricular outflow tract tachycardia. Pacing Clin Electrophysiol 1997; 20: 2188-2192.

[24] Bogun F, Taj M, Ting M, Kim HM, Reich S, Good E, Jongnarangsin K, Chugh A, Pelosi F, Oral H and Morady F. Spatial resolution of pace mapping of idiopathic ventricular tachycardia/ectopy originating in the right ventricular outflow tract. Heart Rhythm 2008; 5: 339-344.

[25] Bloch Thomsen PE, Johannessen A, Jons C, Hansen TF, Kanters JK, Haarbo J, Hansen J, Christiansen LK, Sogaard P, Saermark K and Antzelevitch C. The role of local voltage potentials in outflow tract ectopy. Europace 2010; 12: 850-860.

[26] Pang X, Cheng K, Xu Y, Chen QX, Ling YL and Zhu WQ. Retrospective study of the electrophysiological characteristics and criteria of ablation target for ventricular arrhythmia originating from right ventricular outflow tract. China J Aardiac Arrhymia 2018; 22: 466-471.

[27] Huang LH, Gao MY, Zeng LJ, Xie BQ, Shi L, Wang YJ, Yin XD, Wang YX, Liu XQ, Tian Y, Yang XC and Liu XP. Role of the notched unipolar electrogram in guiding catheter ablation of frequent premature ventricular contractions originating from the ventricular outflow tract. J Int Med Res 2020; 48: 300060520977634.

[28] Liao Z, Zhan X, Wu S, Xue Y, Fang X, Liao H, Deng H, Liang Y, Wei W, Liu Y and Ouyang F. Idiopathic ventricular arrhythmias originating from the pulmonary sinus cusp: prevalence, electrocardiographic/electrophysiological characteristics, and catheter ablation. J Am Coll Cardiol 2015; 66: 2633-2644.

[29] Yang Y, Liu Q, Liu Z and Zhou S. Treatment of pulmonary sinus cusp-derived ventricular arrhythmia with reversed U-curve catheter ablation. J Cardiovasc Electrophysiol 2017; 28: 768-775.

[30] Zhang J, Tang C, Zhang Y and Su X. Pulmonary sinus cusp mapping and ablation: a new concept and approach for idiopathic right ventricular outflow tract arrhythmias. Heart Rhythm 2018; 15: 38-45.

[31] Gami AS, Noheria A, Lachman N, Edwards WD, Friedman PA, Talreja D, Hammill SC, Munger TM, Packer DL and Asirvatham SJ. Anatomical correlates relevant to ablation above the semilunar valves for the cardiac electrophysiologist: a study of 603 hearts. J Interv Card Electrophysiol 2011; 30: 5-15.

[32] Liu CF, Cheung JW, Thomas G, Ip JE, Markowitz SM and Lerman BB. Ubiquitous myocardial extensions into the pulmonary artery demonstrated by integrated intracardiac echocardiography and electroanatomic mapping: changing the paradigm of idiopathic right ventricular outflow tract arrhythmias. Circ Arrhythm Electrophysiol 2014; 7: 691-700.